with biotinylated horse anti-mouse IgG and the ABC-Elite reagent. In all cases 3,3′-diaminobenzidine (with nickel chloride enhancement for SP-C and CC10 staining) was used as the chromagen and sections were counterstained with methyl green.

Analysis of Env RNA expression in lung and airways

Total RNA was isolated from lung, from trachea and from epithelial tissue scraped from the inside of the nose, by using a Polytron tissue homogenizer (Brinkmann) and Trizol RNA isolation reagent (Invitrogen). Samples were treated with DNase and with reverse transcriptase in the presence of a 3′ Env primer; they were then subjected to 30 cycles of PCR amplification with primers flanking the intron in ARJenv (Fig. 1). Products were subjected to electrophoresis in agarose gels and were stained with ethidium bromide.

1. Fan, H. (ed.) *Jaagsiekte Sheep Retrovirus and Lung Cancer* (Springer, Berlin, 2003).
2. Rai, S. K. *et al.* Candidate tumor suppressor HYAL2 is a glycosylphosphatidylinositol (GPI)-anchored cell-surface receptor for jaagsiekte sheep retrovirus, the envelope protein of which mediates oncogenic transformation. *Proc. Natl Acad. Sci. USA* **98,** 4443–4448 (2001).
3. Spencer, T. E., Mura, M., Gray, C. A., Griebel, P. J. & Palmarini, M. Receptor usage and fetal expression of ovine endogenous betaretroviruses: implications for coevolution of endogenous and exogenous retroviruses. *J. Virol.* **77,** 749–753 (2003).
4. Summers, C. *et al.* Systemic immune responses following infection with Jaagsiekte sheep retrovirus and in the terminal stages of ovine pulmonary adenocarcinoma. *J. Gen. Virol.* **83,** 1753–1757 (2002).
5. Sharp, J. M., Angus, K. W., Gray, E. W. & Scott, F. M. Rapid transmission of sheep pulmonary adenomatosis (jaagsiekte) in young lambs. Brief report. *Arch. Virol.* **78,** 89–95 (1983).
6. Maeda, N., Palmarini, M., Murgia, C. & Fan, H. Direct transformation of rodent fibroblasts by jaagsiekte sheep retrovirus DNA. *Proc. Natl Acad. Sci. USA* **98,** 4449–4454 (2001).
7. Allen, T. E. *et al.* The jaagsiekte sheep retrovirus envelope gene induces transformation of the avian fibroblast cell line DF-1 but does not require a conserved SH2 binding domain. *J. Gen. Virol.* **83,** 2733–2742 (2002).
8. Liu, S.-L. & Miller, A. D. Transformation of Madin–Darby canine kidney (MDCK) epithelial cells by sheep retrovirus envelope proteins. *J. Virol.* **79,** 927–933 (2004).
9. Palmarini, M. *et al.* A phosphatidylinositol 3-kinase docking site in the cytoplasmic tail of the Jaagsiekte sheep retrovirus transmembrane protein is essential for envelope-induced transformation of NIH 3T3 cells. *J. Virol.* **75,** 11002–11009 (2001).
10. Liu, S.-L., Lerman, M. I. & Miller, A. D. Putative phosphatidylinositol 3-kinase (PI3K) binding motifs in ovine betaretrovirus Env proteins are not essential for rodent fibroblast transformation and PI3K/Akt activation. *J. Virol.* **77,** 7924–7935 (2003).
11. Danilkovitch-Miagkova, A. *et al.* Hyaluronidase 2 negatively regulates RON receptor tyrosine kinase and mediates transformation of epithelial cells by jaagsiekte sheep retrovirus. *Proc. Natl Acad. Sci. USA* **100,** 4580–4585 (2003).
12. Halbert, C. L., Allen, J. M. & Miller, A. D. Adeno-associated virus type 6 (AAV6) vectors mediate efficient transduction of airway epithelial cells in mouse lungs compared to that of AAV2 vectors. *J. Virol.* **75,** 6615–6624 (2001).
13. Allen, J. M., Halbert, C. L. & Miller, A. D. Improved adeno-associated virus vector production with transfection of a single helper adenovirus gene, E4orf6. *Mol. Ther.* **1,** 88–95 (2000).
14. Malkinson, A. M. The genetic basis of susceptibility to lung tumors in mice. *Toxicology* **54,** 241–271 (1989).
15. Platt, J. A., Kraipowich, N., Villafane, F. & DeMartini, J. C. Alveolar type II cells expressing jaagsiekte sheep retrovirus capsid protein and surfactant proteins are the predominant neoplastic cell type in ovine pulmonary adenocarcinoma. *Vet. Pathol.* **39,** 341–352 (2002).
16. Rai, S. K., DeMartini, J. C. & Miller, A. D. Retrovirus vectors bearing jaagsiekte sheep retrovirus Env transduce human cells by using a new receptor localized to chromosome 3p21.3. *J. Virol.* **74,** 4698–4704 (2000).
17. Liu, S.-L., Duh, F.-M., Lerman, M. I. & Miller, A. D. Role of virus receptor Hyal2 in oncogenic transformation of rodent fibroblasts by sheep betaretrovirus env proteins. *J. Virol.* **77,** 2850–2858 (2003).
18. Miller, A. D., Van Hoeven, N. S. & Liu, S.-L. Transformation and scattering activities of the receptor tyrosine kinase RON/Stk in rodent fibroblasts and lack of regulation by the jaagsiekte sheep retrovirus receptor, Hyal2. *BMC Cancer* **4,** 64 (2004).
19. Fisher, G. H. *et al.* Development of a flexible and specific gene delivery system for production of murine tumor models. *Oncogene* **18,** 5253–5260 (1999).
20. De las Heras, M. *et al.* Evidence for a protein related immunologically to the jaagsiekte sheep retrovirus in some human lung tumours. *Eur. Respir. J.* **16,** 330–332 (2000).
21. Yousem, S. A., Finkelstein, S. D., Swalsky, P. A., Bakker, A. & Ohori, N. P. Absence of jaagsiekte sheep retrovirus DNA and RNA in bronchioloalveolar and conventional human pulmonary adenocarcinoma by PCR and RT-PCR analysis. *Hum. Pathol.* **32,** 1039–1042 (2001).
22. Hiatt, K. M. & Highsmith, W. E. Lack of DNA evidence for jaagsiekte sheep retrovirus in human bronchioloalveolar carcinoma. *Hum. Pathol.* **33,** 680 (2002).
23. Halbert, C. L., Allen, J. M. & Miller, A. D. Efficient mouse airway transduction following recombination between AAV vectors carrying parts of a larger gene. *Nature Biotechnol.* **20,** 697–701 (2002).
24. Halbert, C. L. *et al.* Transduction by adeno-associated virus vectors in the rabbit airway: efficiency, persistence, and readministration. *J. Virol.* **71,** 5932–5941 (1997).

Activation of the DNA damage checkpoint and genomic instability in human precancerous lesions

Vassilis G. Gorgoulis[1]*, **Leandros-Vassilios F. Vassiliou**[1]*, **Panagiotis Karakaidos**[1], **Panayotis Zacharatos**[1], **Athanassios Kotsinas**[1], **Triantafillos Liloglou**[2], **Monica Venere**[3,4], **Richard A. DiTullio Jr**[3,4], **Nikolaos G. Kastrinakis**[1], **Brynn Levy**[6], **Dimitris Kletsas**[7], **Akihiro Yoneta**[3], **Meenhard Herlyn**[3], **Christos Kittas**[1] & **Thanos D. Halazonetis**[3,5]

[1]*Department of Histology and Embryology, School of Medicine, University of Athens, Athens GR-11527, Greece*
[2]*Roy Castle Lung Cancer Research Programme, Cancer Research Center, University of Liverpool, Liverpool L3 9TA, UK*
[3]*The Wistar Institute, Philadelphia, Pennsylvania 19104-4268, USA*
[4]*Graduate Group in Biomedical Sciences and*
[5]*Department of Pathology and Laboratory Medicine, University of Pennsylvania, Philadelphia, Pennsylvania 19104, USA*
[6]*Department of Human Genetics, Mount Sinai School of Medicine, New York, New York 10029, USA*
[7]*Institute of Biology, National Centre of Scientific Research 'Demokritos', Athens GR-15310, Greece*

* These authors contributed equally to this work

DNA damage checkpoint genes, such as *p53*, are frequently mutated in human cancer, but the selective pressure for their inactivation remains elusive[1–3]. We analysed a panel of human lung hyperplasias, all of which retained wild-type *p53* genes and had no signs of gross chromosomal instability, and found signs of a DNA damage response, including histone H2AX and Chk2 phosphorylation, p53 accumulation, focal staining of p53 binding protein 1 (53BP1) and apoptosis. Progression to carcinoma was associated with *p53* or *53BP1* inactivation and decreased apoptosis. A DNA damage response was also observed in dysplastic nevi and in human skin xenografts, in which hyperplasia was induced by overexpression of growth factors. Both lung and experimentally-induced skin hyperplasias showed allelic imbalance at loci that are prone to DNA double-strand break formation when DNA replication is compromised (common fragile sites). We propose that, from its earliest stages, cancer development is associated with DNA replication stress, which leads to DNA double-strand breaks, genomic instability and selective pressure for *p53* mutations.

The most frequently mutated gene in human cancer is *p53*, a gene that functions in the checkpoint response to DNA double-strand breaks (DSBs; Fig. 1a)[1,2]. Several models (not mutually exclusive) have been proposed to explain the high frequency of *p53* inactivation[3–6]. One of the prevailing models states that tumour growth leads to telomere attrition and hypoxia, resulting in a DNA damage response[4–6]. This model predicts that the DNA damage response occurs some time after cancer initiation[3]. Here, we performed a systematic analysis of precancerous and cancer lesions to determine how early during human cancer development a DNA DSB checkpoint response might become apparent.

We first examined a previously described panel of surgically-resected, non-small cell lung carcinomas (NSCLCs) from patients who had received no form of cancer therapy before surgery[7,8]. Almost all specimens in this panel ($n = 74$) contained normal adjacent lung tissue ($n = 72$), and some also contained hyperplastic ($n = 17$) and dysplastic lesions ($n = 2$), the location of which suggested that they were precursors of the NSCLCs. The *p53* gene was wild-type in all of the hyperplasias, mutant in the dysplasias, and either mutant ($n = 45$) or wild-type ($n = 29$) in the NSCLCs. For the two dysplasias, the same *p53* mutations were found in the adjacent NSCLCs, consistent with the dysplasias being precursors of the adjacent NSCLCs (data not shown).

The occurrence of a DNA damage response can be ascertained by monitoring histone H2AX phosphorylation (γ-H2AX), 53BP1 intracellular localization, Chk2 phosphorylation (on Thr 68) and p53 protein levels[9–13] (Fig. 1a). In the normal lung epithelium, all markers were consistent with the absence of a DNA damage response (Fig. 1b). However, in the hyperplasias there were signs that the DNA DSB checkpoint pathway had been activated. 53BP1, which is a sensor of DNA DSBs[14], was localized to discrete nuclear foci. This is reminiscent of the 53BP1 foci that are observed in irradiated tissue culture cells and represent sites of DNA DSBs[12]. In addition, histone H2AX and Chk2 were phosphorylated, p53 protein levels were elevated, and some cells were undergoing apoptosis (Fig. 1b). In the dysplasias and NSCLCs there were also signs of a DNA damage response, shown by 53BP1 localization and histone H2AX and Chk2 phosphorylation. However, apoptosis was suppressed relative to the hyperplasias. In most cases this suppression was associated with *p53* mutations or with low levels of wild-type p53 protein (Fig. 1b and 2). In a small number of NSCLCs, decreased apoptosis was associated with low levels of 53BP1 mRNA and protein (Fig. 1c, d and 2). In these NSCLCs, Chk2 was not phosphorylated on Thr 68, but histone H2AX phosphorylation persisted (Fig. 1c and 2). These effects of low 53BP1 expression in NSCLCs replicate the effects of 53BP1 depletion in tissue culture cells[13,15] (Supplementary Fig. 1).

To expand these studies to other tumour types, we examined a cohort of patients with malignant melanoma ($n = 61$). Eleven of these patients also had dysplastic nevi (nevi with melanocytic hyperplasia and atypia) adjacent to their melanoma. All of the dysplastic nevi, most of which were from areas of the body not exposed to sunlight, stained positive for phosphorylated histone
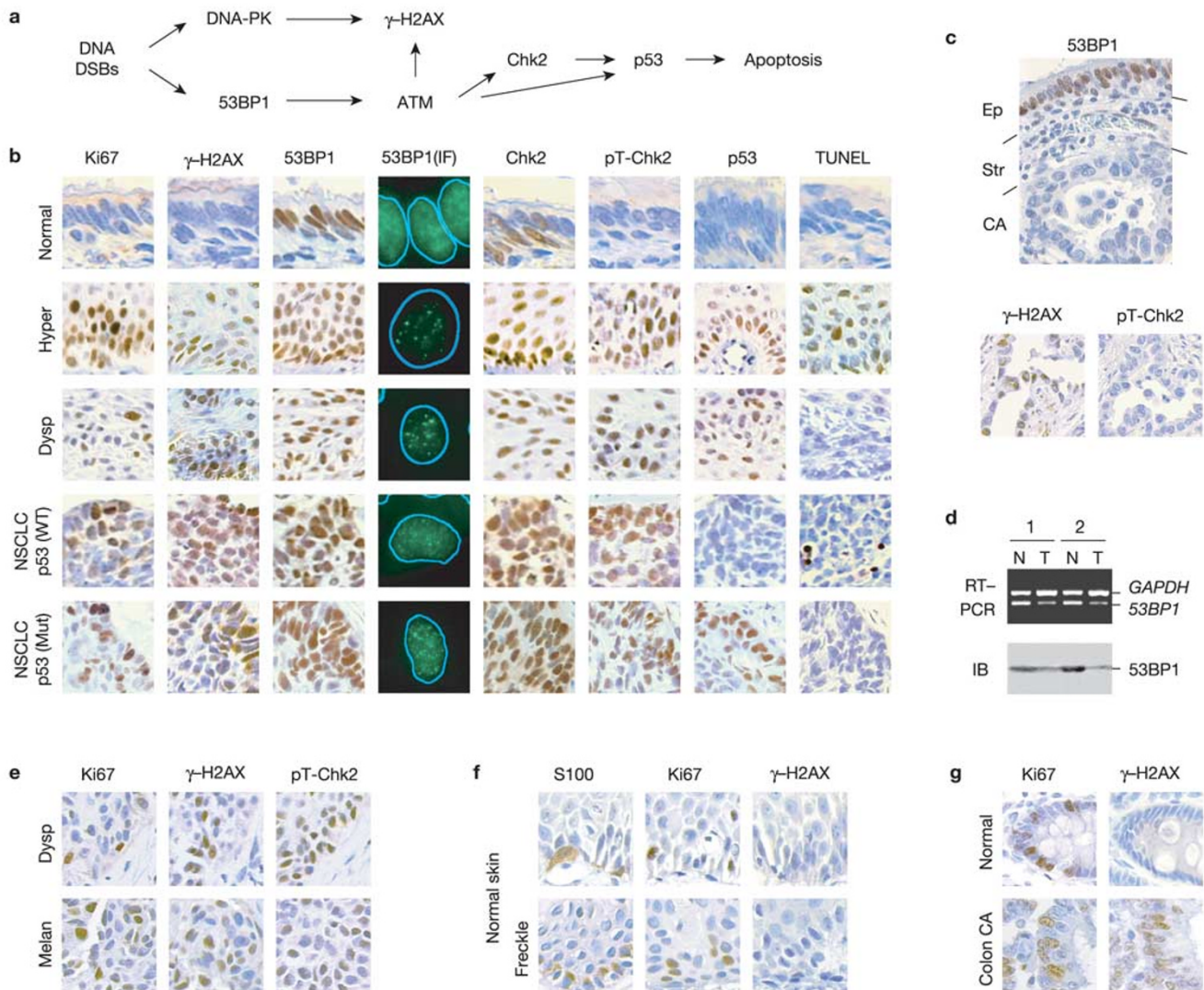
Figure 1 Activation of the DNA double-strand break (DSB) checkpoint pathway in human preneoplastic and neoplastic lesions. **a**, Current model of DNA DSB signalling pathway leading to p53-dependent apoptosis. For clarity, only a subset of the DNA DSB-response proteins are shown. DNA-PK, DNA-dependent protein kinase. **b**, Immunohistochemistry of normal bronchial epithelium, hyperplastic (Hyper), dysplastic (Dysp) and non-small cell lung carcinoma (NSCLC) lesions. p53(WT) and p53(Mut) are wild-type and mutant *p53* genotypes, respectively. Ki67 and TUNEL staining were used to calculate proliferation and apoptotic indices, respectively. γ-H2AX, phosphorylated H2AX; pT-Chk2, Chk2 phosphorylated on Thr 68. The distribution of 53BP1 in cells was examined by immunofluorescence (IF): 53BP1 is shown in green, nuclei are outlined in blue. **c**, Immunohistochemistry of a NSCLC that does not express 53BP1. Upper panel, a section showing normal epithelium (Ep), stroma (Str) and NSCLC (CA) stained for 53BP1. Lower panels, adjacent NSCLC sections stained for γ-H2AX and pT-Chk2. **d**, Reverse transcriptase PCR (RT–PCR) and immunoblot (IB) analysis of two NSCLC lesions that stained negative for 53BP1 by immunohistochemistry. N, normal tissue; T, tumour tissue; *GAPDH*, glyceraldehyde-3-phosphate dehydrogenase. **e**, Immunohistochemistry of a dysplastic nevus (Dysp) and melanoma (Melan) from the same patient. **f**, Immunohistochemistry of two areas of normal skin adjacent to the dysplastic nevus shown in (**e**). One of the areas of normal skin (lower panels) corresponds to a freckle (simple lentigo). S100 staining marks the melanocytes. **g**, Immunohistochemistry of normal colonic epithelium and colon carcinoma (CA) from the same patient.

H2AX and Chk2 (Fig. 1e and 2), whereas the adjacent skin always stained negative (Fig. 1f). The melanomas also stained positive for phosphorylated histone H2AX and Chk2, with the exception of a small number of melanomas, which stained positive for γ-H2AX but negative for phosphorylated Chk2. These latter melanomas did not express either 53BP1 ($n = 5$) or Chk2 ($n = 6$) protein (Fig. 2). Unlike the lung hyperplasias, the percentage of apoptotic cells in the dysplastic nevi was low and did not decrease during progression to melanoma. Instead, progression to melanoma was associated with an increase in the proliferation index (Fig. 2). Although several models can be used to explain the increased proliferation that accompanies progression from dysplastic nevi to melanoma, one possibility is that activation of the DNA damage checkpoint in dysplastic nevi induces cell cycle arrest, and that progression to melanoma is associated with escape from this arrest through various mechanisms (including suppression of 53BP1 and Chk2 expression). In support of this model, dysplastic nevi stained positive for Cdc2 phosphorylated on Tyr 15 (Supplementary Fig. 2), which is a marker of G2 checkpoint activation[2,11].

The results presented above, as well as similar and complementary findings from another research group[16], suggest that the DNA damage checkpoint is activated in a wide variety of human preneoplastic and neoplastic lesions. However, it is formally possible that the markers studied above would stain positive during normal cell proliferation, in which case the response of the preneoplastic and neoplastic lesions could simply be a reflection of their high proliferation index (Fig. 2). To explore this possibility we examined normal colonic crypts in surgically resected tissues from colon cancer patients. Despite having a higher proliferation index than the lung and melanocytic preneoplastic and neoplastic lesions, normal colonic epithelium ($n = 20$) stained uniformly negative for both histone H2AX and Chk2 phosphorylation (Fig. 1g and 2). Normal skin, which has a relatively high proliferation index, also stained negative (Fig. 1f and data not shown). Thus, activation of the DNA damage checkpoint occurs specifically in preneoplastic and neoplastic lesions.

The lung hyperplasias and dysplastic nevi that we studied are very early lesions in terms of the stage of cancer development, but they were probably precursors of the adjacent NSCLCs (see below) and melanomas, respectively. Because cancer can take years to develop, it is possible that the preneoplastic lesions did not show a DNA damage response when first formed. To address this issue we studied a model of hyperplasia[17] in which human skin xenografts were implanted on the backs of immunodeficient mice and then induced to become hyperplastic by weekly subcutaneous injections (over 4 weeks) of adenoviral vectors expressing growth factors (basic fibroblast growth factor, stem cell factor and endothelin-3). Control xenografts were either not injected or injected with an adenovirus expressing green fluorescent protein (GFP). Both newborn human foreskin and adult skin (from breast reduction cosmetic surgeries) were grafted. Foreskin from a specific donor, owing to its small size, was grafted on a single mouse, such that the various treatment groups consisted of grafts from different individuals. The larger adult skin samples were each used to prepare two grafts; one was injected with adenoviruses expressing growth factors, and the other served as a donor-matched untreated control. All grafts were harvested for analysis one week after the final injection.

Both the foreskin- and adult skin-derived hyperplastic xenografts mimicked the lung hyperplasias in terms of DNA damage response: 53BP1 was localized to discrete nuclear foci, histone H2AX and Chk2 were phosphorylated, p53 protein levels were induced and there was evidence of apoptosis (Fig. 3). None of these effects was observed in the non-injected controls or the controls injected with the adenovirus expressing GFP (Fig. 3e).

One possible mechanism for activation of the DNA damage checkpoint in the precancerous human lesions and hyperplastic skin xenografts might involve telomere attrition. We therefore compared telomere lengths in matched control and hyperplastic adult skin xenograft pairs. No differences between the groups were observed, but shortened telomeres were apparent in the K562 erythroleukaemia cancer cell line (Fig. 3d). The absence of telomere attrition, at least at this level of analysis, is perhaps not surprising given that the xenografts were obtained from newborns and young adults, and were examined just a few weeks after grafting.

Another possible mechanism for the DNA damage response observed in the precancerous lesions might involve replication stress. We noted high levels of cyclin E protein in both the lung hyperplasias and hyperplastic human skin xenografts (Supplementary Fig. 3 and data not shown). High levels of cyclin E, and more generally, deregulation of cyclin-dependent kinase activity in G1, are very frequent in human cancer, and compromise prereplication complex assembly and licensing of origins of replication. As a result, too few origins may fire or some origins may fire more than once per cell cycle. This would lead to replication stress, which in turn could lead to DNA DSBs, activation of the DNA damage checkpoint and even genomic instability[18–22].

As a first step in linking replication stress to the DNA damage response observed in preneoplasia and neoplasia, we studied cancer cell lines such as the Saos2 osteosarcoma and HeLa cervical carcinoma lines, in which the DNA damage checkpoint is active even in the absence of exposure to ionizing radiation[15]. If the DNA damage response in these cell lines is due to replication stress, it should be dependent on entry into S phase. Furthermore, the γ-H2AX foci in the nuclei of these cells should colocalize with ATR (ATM-Rad3-related protein)–ATRIP (ATR-interacting protein) foci because the ATR–ATRIP complex is recruited to sites of DNA replication stress[23,24]. Both of these predictions were found to
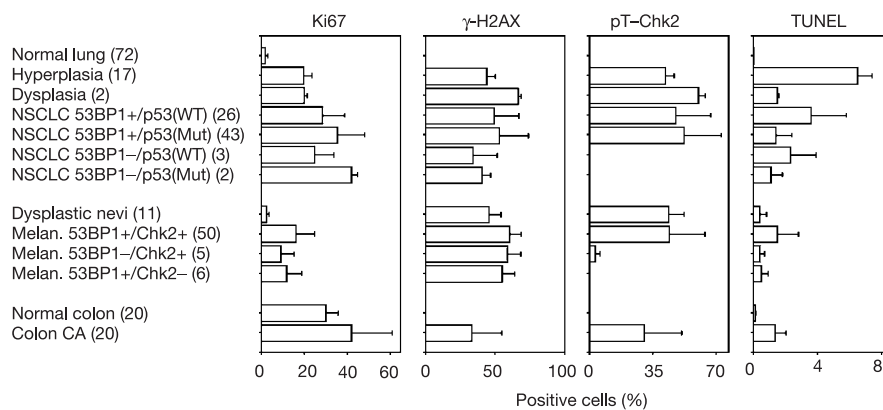

Figure 2 Summary of DNA double-strand break responses in human normal tissues, preneoplastic lesions and neoplastic lesions. The numbers in parentheses indicate the number of samples examined. The bars show the mean ± s.d. of the percentage of cells that stained positive for the indicated marker.

be true. Saos2 cells stably transfected with a doxycycline-inducible *p21/WAF1/CDKN1A* gene were synchronized in G1 by inducing expression of *p21/WAF1/CDKN1A*, and then released into S phase by doxycycline withdrawal. Histone H2AX phosphorylation was more robust in cycling cells than in the cells arrested in G1, consistent with similar results by others[25]. However, in early passage human diploid lung fibroblasts, histone H2AX was unphosphorylated, irrespective of whether the cells were cycling or resting (Supplementary Fig. 4a). Furthermore, a majority of γ-H2AX foci in non-irradiated Saos2 and HeLa cells were found to colocalize with ATRIP foci; as a control, γ-H2AX foci induced in these cell lines in response to ionizing radiation were devoid of ATRIP (Supplementary Fig. 4b).

To identify evidence for replication stress in preneoplastic human lesions, we reasoned that replication stress could lead to allelic imbalances, through formation of DNA DSBs and defective DNA repair. The loci in the genome that are prone to DNA DSB formation under conditions of replication stress are called common fragile sites[26,27]. We predicted that these sites would be preferentially targeted for allelic imbalance in human preneoplastic lesions, and

tested this hypothesis using genomic DNA isolated from normal lung, hyperplastic and neoplastic tissue from 11 NSCLC patients. Allelic imbalance at the most common fragile site (*FRA3B* on chromosome 3p14) was compared to loci on chromosomes that commonly show allelic imbalance in advanced human cancers but do not correspond to common fragile sites. In the hyperplasias, allelic imbalance affecting the common fragile site *FRA3B* was very frequent (and occasionally extended to more distant loci on 3p), whereas the other chromosomal loci were either minimally affected or not affected (Fig. 4a). Consistent with preferential targeting of common fragile sites in these hyperplasias, comparative genomic hybridization analysis also revealed the absence of gross chromosomal instability (Supplementary Fig. 5 and data not shown). In the NSCLCs, allelic imbalances established in the hyperplastic stage persisted (providing evidence for progression from hyperplasia to NSCLC), but additional allelic imbalances affecting known tumour suppressor loci were also present, as was gross chromosomal instability (Fig. 4a, Supplementary Fig. 6 and data not shown). These and similar results[16,28–30] are consistent with the presence of replication stress in human preneoplastic lesions.
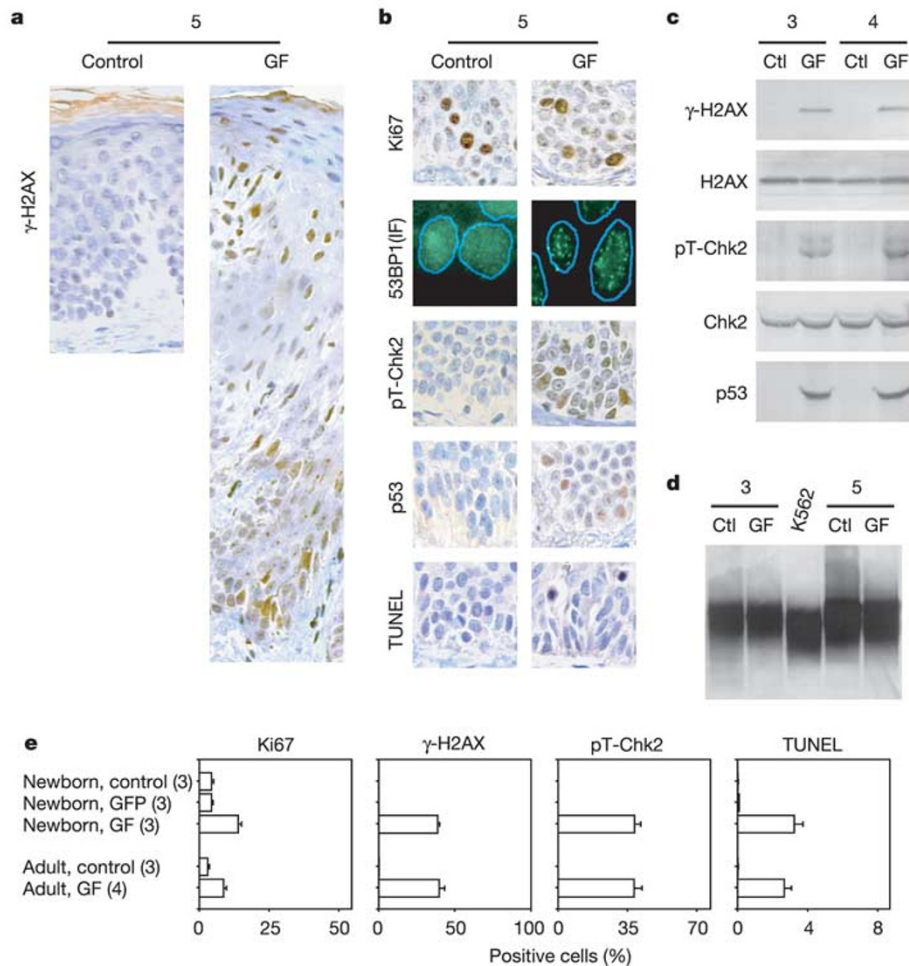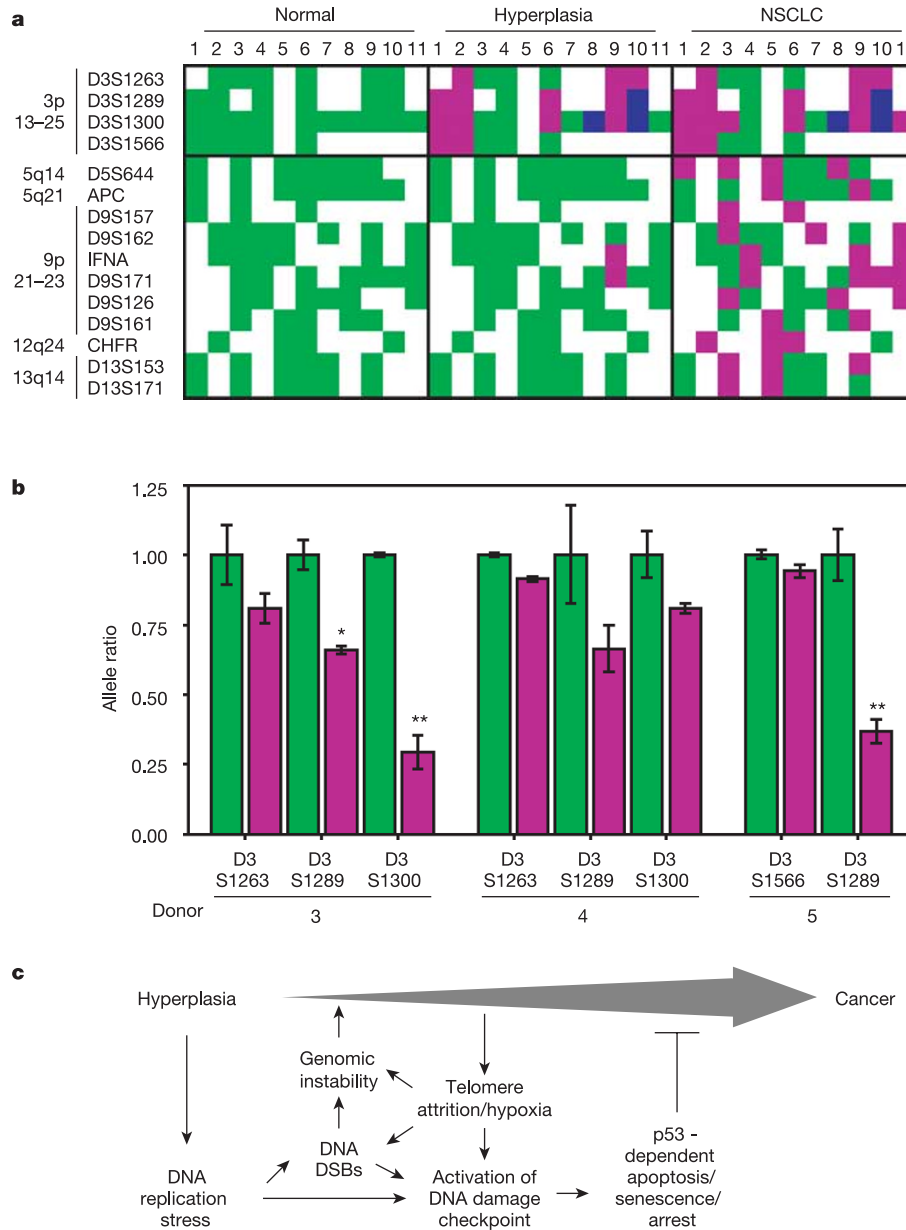

Figure 3 Activation of the DNA DSB checkpoint pathway in experimentally induced hyperplasias. Human newborn foreskin or adult skin xenografts were either untreated (control, Ctl), injected with an adenoviral vector that expresses GFP, or injected with adenoviral vectors overexpressing growth factors (GF). **a**, Cross-section of the entire epithelium of control and growth-factor-treated adult skin xenografts from the same donor (number 5), stained for γ-H2AX. **b**, Immunohistochemistry of control and growth factor-treated adult skin xenografts from donor 5 for Ki67, pT-Chk2 (Chk2 phosphorylated on Thr 68) and p53. TUNEL staining was used to mark the apoptotic cells and immunofluorescence (IF) was used to monitor the intracellular localization of 53BP1.

c, Immunoblot analysis of extracts prepared from control and growth factor-treated adult skin xenografts (from donors 3 and 4) to monitor H2AX and Chk2 phosphorylation (γ-H2AX and pT-Chk2, respectively) and p53 protein levels. **d**, Telomere length of control and growth-factor-treated adult skin xenografts from donors 3 and 5, assessed by Southern blot analysis. The erythroleukaemia cell line K562 was used as a control. **e**, Summary of DNA DSB responses in newborn foreskin and adult skin xenografts. Numbers in parentheses indicate the number of xenografts examined. The bars show the mean ± s.d. of the percentage of cells in each xenograft that stained positive for the indicated marker.

We extended the analysis of allelic imbalance at common fragile sites to the matched pairs of control and hyperplastic adult skin xenografts. Genomic DNA was isolated from 2–5 serial sections of xenograft tissue, and allelic imbalance was examined using two microsatellite markers (D3S1289 and D3S1300) that map to the *FRA3B* common fragile site on chromosome 3p, together with two markers (D3S1263 and D3S1566) that map to non-fragile sites on

chromosome 3p (3p25 and 3p13, respectively). In all three matched pairs examined, allelic imbalance at *FRA3B* was evident in the hyperplastic xenograft, whereas the 3p25 and 3p13 loci remained heterozygous (Fig. 4b). Thus, in an experimental human skin model, aberrant growth factor signalling associated with loss of tissue homeostasis (hyperplasia) can lead to allelic imbalance at common fragile sites within a few weeks.

Figure 4 Allelic imbalance at common fragile sites in early human cancer lesions and model for activation of the DNA DSB checkpoint in cancer. **a**, Allelic imbalance at the common fragile site *FRA3B* on chromosome 3p14 is frequent in lung hyperplasias and precedes allelic imbalance at other loci. Allelic imbalance analysis of normal bronchial epithelium, hyperplastic and neoplastic tissue from 11 NSCLC patients. The microsatellite markers used in the analysis and their chromosomal position are indicated on the left. Markers D3S1289 and D3S1300 map to *FRA3B*; marker D3S1263 maps to 3p25; and marker D3S1566 maps to 3p13. Heterozygous loci (green), allelic imbalance (pink), microsatellite instability (blue), non-informative (homozygous) loci (white). **b**, Allelic imbalance at the common fragile site *FRA3B* in human adult skin xenografts. Data shown are means ± s.e.m. of allele ratios for microsatellite markers D3S1263, D3S1289, D3S1300 and D3S1566 from control (green) and growth-factor-treated (pink) xenografts from donors 3, 4 and 5. Ratios are not shown for non-informative (homozygous) loci. The

allele ratios were determined from two independent PCR reactions per sample and scaled so that the ratio would be 1 for the control xenografts. Asterisks indicate significantly different allele ratios between the control and growth factor-treated xenografts (single asterisk, $P < 0.005$; double asterisk, $P < 0.001$). In the matched pair from donor 4, the decrease in the allele ratio for marker D3S1289 in the hyperplastic xenograft reached statistical significance when tested using the mean variance, but not when tested using the individual variance. **c**, Model for activation of the DNA damage checkpoint in cancer. Aberrant stimulation of cell proliferation (as occurs in preneoplastic lesions) leads to DNA replication stress, DNA DSBs, genomic instability, activation of the DNA damage checkpoint, and p53-dependent apoptosis. p53-dependent apoptosis suppresses expansion of the precancerous lesion (*p53* tumour suppressor function) and provides selective pressure for *p53* inactivation. Telomere attrition and hypoxia can also contribute to DNA DSB formation, activation of the checkpoint and genomic instability.

Our findings, together with an accompanying study[16], suggest a model that might explain the tumour suppressor function of *p53* and also hint to mechanisms leading to genomic instability in early cancer lesions (Fig. 4c). We propose that in precancerous lesions, aberrant stimulation of cell proliferation leads to DNA replication stress. This stress, either directly or through the formation of DNA DSBs, can activate the DNA damage checkpoint, which in turn induces cell cycle arrest or apoptosis, and thus functions as a tumour suppressor. In those cells that do not undergo permanent cell cycle arrest or apoptosis, there is a likelihood that errors in DNA DSB repair will lead to allelic imbalances. These imbalances will preferentially target common fragile sites because these sites are most sensitive to replication stress. At later stages, telomere attrition and hypoxia will also contribute to checkpoint activation and genomic instability[4–6]. Eventually, tumour suppressor loci (such as *p53*) will be targeted, releasing the cells from the suppressive effects of the DNA damage checkpoint pathway and facilitating tumour progression. □

Methods

Antibodies

For immunohistochemistry, immunofluorescence and immunoblot analysis we used previously characterized primary antibodies[13–15] at the indicated dilutions: anti-phospho-H2AX (Ser 139) (1:100; Upstate); anti-53BP1 and anti-Chk2 (hybridoma supernatants, 1:20; refs 13–15); anti-phospho-Chk2 (Thr 68, Lot 1) (1:100; Cell Signalling Technology); anti-p53 (DO7) (1:100; Dako); anti-Ki67 (MIB-1) (1:100; Dako); and anti-S100 (1:100; Dako).

Tissue samples

Our database of frozen and formalin-fixed, paraffin-embedded material from a total of 74 resected NSCLCs, and adjacent normal lung tissue and corresponding precancerous lesions (17 cases of hyperplasias/metaplasias, with two cases also bearing dysplasias) has previously been described[7,8]. Sixty-one cases of sporadic malignant melanoma, 11 of which developed from dysplastic nevi, and 20 non-familial colon carcinoma cases were selected without bias from the patient population of the Agios Savas Hospital in Athens, Greece. None of the patients had undergone cancer therapy before surgical resection of the lesions.

Human skin xenograft model

The human skin xenograft model has been described[17]. For these studies, we examined 9 newborn foreskin xenografts: 3 were injected subcutaneously with adenoviruses expressing basic fibroblast growth factor, stem cell factor and endothelin-3; 3 were injected with an adenovirus expressing GFP; and 3 were left untreated. Injections were weekly over a period of 4 weeks. We also studied 4 adult skin grafts from patients undergoing breast reduction cosmetic surgeries. These grafts were cut in half, and each half was implanted in a separate SCID mouse. For each graft, one mouse received injections with adenoviral vectors expressing the growth factors listed above, and in the other mouse the graft was untreated. All grafts were harvested a week after the last injection. The foreskin grafts were fixed with formalin and analysed by immunohistochemistry. Part of each adult skin graft was flash-frozen and used to prepare protein extracts, and another part was fixed with formalin and analysed by immunohistochemistry or used to prepare genomic DNA. One of the adult untreated grafts was damaged during sectioning and was not analysed by immunohistochemistry.

Analysis of tissue samples

Formalin-fixed tissue sections were processed for immunohistochemistry, immunofluorescence and Tdt-mediated dUTP nick-end labelling (TUNEL) analysis as previously described[7,8]. RNA was extracted from frozen samples and used to prepare complementary DNA[7,8]. For analysis of *53BP1* (also known as *TP53BP1*) expression at the mRNA level, the cDNA was amplified by semiquantitative multiplex polymerase chain reaction (PCR) using primers specific for *53BP1* (forward primer 3′-GCAGCCTCTGTGAA GCAGCA-5′; reverse 3′-ATGCAAGGAATCCAGTTACACACAA-5′) and *GAPDH* (*GAPD*), as standard[7,8]. *p53* mutations were identified by single-strand conformation polymorphism analysis and by sequencing[7,8]. Proteins were extracted by lysis of minced frozen samples using RIPA buffer supplemented with protease inhibitors[13]. Histones were isolated from the RIPA-insoluble pellet by extraction with buffer consisting of 10 mM HEPES, 1.5 mM $MgCl_2$, 10 mM KCl, 0.5 mM dithiothreitol, 1.5 mM phenylmethyl sulphonyl fluoride and 0.25 N HCl for 1 h at 4 °C. Immunoblotting was performed as previously described[13].

Telomere length assay

Telomere lengths were determined using the TeloTAGGG Telomere Length Assay (Roche Diagnostics) according to the manufacturer's instructions. Briefly, 4 μg genomic DNA isolated from two matched pairs of control and growth factor-treated adult skin xenografts was digested with *Hinf*I and *Rsa*I, and subjected to Southern blot analysis using telomere-specific labelled probes. DNA prepared from the K562 erythroleukaemic cell line served as a control.

Allelic imbalance analysis

Allelic imbalance analysis of lung tissues was tabulated from our previously published studies (refs 7, 8 and references therein), or extended to include microsatellite markers for chromosome 3p. For analysis of human skin xenografts, 2–5 serial 10 μm-thick paraffin-embedded sections were microdissected using laser capture, and genomic DNA was extracted as previously described[7]. Each genomic DNA sample was subjected to two independent PCR reactions, and the PCR products were resolved using a 377 ABI PRISM automated sequencer (Applied Biosystems), as previously described[8]. Differences in allele ratios between control and growth factor-treated xenografts were evaluated twice for statistical significance (using the individual variances and the mean variance calculated from all the replicates), and were scored positive only if both evaluations showed statistical significance.

1. Hollstein, M., Sidransky, D., Vogelstein, B. & Harris, C. C. p53 mutations in human cancers. *Science* **253**, 49–53 (1991).
2. Kastan, M. B. & Bartek, J. Cell-cycle checkpoints and cancer. *Nature* **432**, 316–323 (2004).
3. Halazonetis, T. D. Constitutively active DNA damage checkpoint pathways as the driving force for the high frequency of p53 mutations in human cancer. *DNA Repair (Amst.)* **3**, 1057–1062 (2004).
4. Takai, H., Smogorzewska, A. & de Lange, T. DNA damage foci at dysfunctional telomeres. *Curr. Biol.* **13**, 1549–1556 (2003).
5. d'Adda di Fagagna, F. *et al.* A DNA damage checkpoint response in telomere-initiated senescence. *Nature* **426**, 194–198 (2003).
6. Graeber, T. G. *et al.* Hypoxia-mediated selection of cells with diminished apoptotic potential in solid tumours. *Nature* **379**, 88–91 (1996).
7. Gorgoulis, V. G. *et al.* Alterations of the p16-pRb pathway and the chromosome locus 9p21–22 in non-small-cell lung carcinomas: relationship with p53 and MDM2 protein expression. *Am. J. Pathol.* **153**, 1749–1765 (1998).
8. Karakaidos, P. *et al.* Overexpression of the replication licensing regulators hCdt1 and hCdc6 characterizes a subset of non-small-cell lung carcinomas: synergistic effect with mutant p53 on tumor growth and chromosomal instability—evidence of E2F-1 transcriptional control over hCdt1. *Am. J. Pathol.* **165**, 1351–1365 (2004).
9. Kastan, M. B., Onyekwere, O., Sidransky, D., Vogelstein, B. & Craig, R. W. Participation of p53 protein in the cellular response to DNA damage. *Cancer Res.* **51**, 6304–6311 (1991).
10. Rogakou, E. P., Pilch, D. R., Orr, A. H., Ivanova, V. S. & Bonner, W. M. DNA double-stranded breaks induce histone H2AX phosphorylation on serine 139. *J. Biol. Chem.* **273**, 5858–5868 (1998).
11. Bartek, J. & Lukas, J. Chk1 and Chk2 kinases in checkpoint control and cancer. *Cancer Cell* **3**, 421–429 (2003).
12. Schultz, L. B., Chehab, N. H., Malikzay, A. & Halazonetis, T. D. p53 binding protein 1 (53BP1) is an early participant in the cellular response to DNA double-strand breaks. *J. Cell Biol.* **151**, 1381–1390 (2000).
13. Mochan, T. A., Venere, M., DiTullio, R. A. Jr & Halazonetis, T. D. 53BP1 and NFBD1/MDC1-Nbs1 function in parallel interacting pathways activating ataxia-telangiectasia mutated (ATM) in response to DNA damage. *Cancer Res.* **63**, 8586–8591 (2003).
14. Huyen, Y. *et al.* Methylated lysine 79 of histone H3 targets 53BP1 to DNA double-strand breaks. *Nature* **432**, 406–411 (2004).
15. DiTullio, R. A. Jr *et al.* 53BP1 functions in an ATM-dependent checkpoint pathway that is constitutively activated in human cancer. *Nature Cell Biol.* **4**, 998–1002 (2002).
16. Bartkova, J. *et al.* DNA damage response as a candidate anti-cancer barrier in early human tumorigenesis. *Nature* doi:10.1038/nature03482 (this issue).
17. Berking, C. *et al.* Induction of melanoma phenotypes in human skin by growth factors and ultraviolet B. *Cancer Res.* **64**, 807–811 (2004).
18. Spruck, C. H., Won, K. A. & Reed, S. I. Deregulated cyclin E induces chromosome instability. *Nature* **401**, 297–300 (1999).
19. Lengronne, A. & Schwob, E. The yeast CDK inhibitor Sic1 prevents genomic instability by promoting replication origin licensing in late G1. *Mol. Cell* **9**, 1067–1078 (2002).
20. Tanaka, S. & Diffley, J. F. Deregulated G1-cyclin expression induces genomic instability by preventing efficient pre-RC formation. *Genes Dev.* **16**, 2639–2649 (2002).
21. Vaziri, C. *et al.* A p53-dependent checkpoint pathway prevents rereplication. *Mol. Cell* **11**, 997–1008 (2003).
22. Ekholm-Reed, S. *et al.* Deregulation of cyclin E in human cells interferes with prereplication complex assembly. *J. Cell Biol.* **165**, 789–800 (2004).
23. Tibbetts, R. S. *et al.* Functional interactions between BRCA1 and the checkpoint kinase ATR during genotoxic stress. *Genes Dev.* **14**, 2989–3002 (2000).
24. Cortez, D., Guntuku, S., Qin, J. & Elledge, S. J. ATR and ATRIP: partners in checkpoint signaling. *Science* **294**, 1713–1716 (2001).
25. MacPail, S. H., Banath, J. P., Yu, Y., Chu, E. & Olive, P. L. Cell cycle-dependent expression of phosphorylated histone H2AX: reduced expression in unirradiated but not X-irradiated G1-irradiated G1-phase cells. *Radiat. Res.* **159**, 759–767 (2003).
26. Arlt, M. F., Casper, A. M. & Glover, T. W. Common fragile sites. *Cytogenet. Genome Res.* **100**, 92–100 (2003).
27. Casper, A. M., Nghiem, P., Arlt, M. F. & Glover, T. W. ATR regulates fragile site stability. *Cell* **111**, 779–789 (2002).
28. Mao, L. *et al.* Frequent microsatellite alterations at chromosomes 9p21 and 3p14 in oral premalignant lesions and their value in cancer risk assessment. *Nature Med.* **2**, 682–685 (1996).
29. Wistuba, I. I. *et al.* High resolution chromosome 3p allelotyping of human lung cancer and preneoplastic/preinvasive bronchial epithelium reveals multiple, discontinuous sites of 3p allele loss and three regions of frequent breakpoints. *Cancer Res.* **60**, 1949–1960 (2000).
30. Maitra, A. *et al.* High-resolution chromosome 3p allelotyping of breast carcinomas and precursor lesions demonstrates frequent loss of heterozygosity and a discontinuous pattern of allele loss. *Am. J. Pathol.* **159**, 119–130 (2001).

Correspondence and requests for materials should be addressed to T.D.H. (halazonetis@wistar.upenn.edu).

....

Specific killing of BRCA2-deficient tumours with inhibitors of poly(ADP-ribose) polymerase

Helen E. Bryant[1], **Niklas Schultz**[2], **Huw D. Thomas**[3], **Kayan M. Parker**[1], **Dan Flower**[1], **Elena Lopez**[1], **Suzanne Kyle**[3], **Mark Meuth**[1], **Nicola J. Curtin**[3] & **Thomas Helleday**[1,2]

[1]*The Institute for Cancer Studies, University of Sheffield, Medical School, Beech Hill Road, Sheffield S10 2RX, UK*
[2]*Department of Genetics, Microbiology and Toxicology, Arrhenius Laboratory, Stockholm University, S-106 91 Stockholm, Sweden*
[3]*Northern Institute for Cancer Research, University of Newcastle upon Tyne, Medical School, Newcastle upon Tyne, NE2 4HH, UK*

....

Poly(ADP-ribose) polymerase (PARP1) facilitates DNA repair by binding to DNA breaks and attracting DNA repair proteins to the site of damage[1–3]**. Nevertheless, PARP1**$^{-/-}$ **mice are viable, fertile and do not develop early onset tumours**[4]**. Here, we show that PARP inhibitors trigger** γ**-H2AX and RAD51 foci formation. We**

propose that, in the absence of PARP1, spontaneous single-strand breaks collapse replication forks and trigger homologous recombination for repair. Furthermore, we show that BRCA2-deficient cells, as a result of their deficiency in homologous recombination, are acutely sensitive to PARP inhibitors, presumably because resultant collapsed replication forks are no longer repaired. Thus, PARP1 activity is essential in homologous recombination-deficient *BRCA2* mutant cells. We exploit this requirement in order to kill BRCA2-deficient tumours by PARP inhibition alone. Treatment with PARP inhibitors is likely to be highly tumour specific, because only the tumours (which are BRCA2$^{-/-}$) in BRCA2$^{+/-}$ patients are defective in homologous recombination. The use of an inhibitor of a DNA repair enzyme alone to selectively kill a tumour, in the absence of an exogenous DNA-damaging agent, represents a new concept in cancer treatment.

Despite its important role in the cellular response to genotoxic stress, PARP1 is not required for survival in the absence of such an insult, and PARP1$^{-/-}$ mice are viable and fertile[2,5,6]. These mice do not develop early onset tumours and tumour latency is increased in PARP1 knockout mice that are deficient for p53 (ref. 4). Nevertheless, it is generally accepted that loss of PARP1 activity is important in maintaining genetic stability, because PARP1$^{-/-}$ mice exhibit defective DNA single-strand break (SSB) repair and an increase in homologous recombination, sister chromatid exchange and micronuclei formation[1,2,5–7]. However, the elevated homologous recombination levels in PARP1$^{-/-}$ mice represent an error-free repair pathway, which may explain why the genetic instability in PARP1-deficient or inhibited cells is not associated with any accumulation of mutations or cancer.

PARP1 does not seem to be directly involved in homologous recombination, as RAD51 foci form normally in PARP1-deficient cells and homologous recombination-mediated repair of a DNA double-strand break (DSB) is unaffected by inhibition or loss of
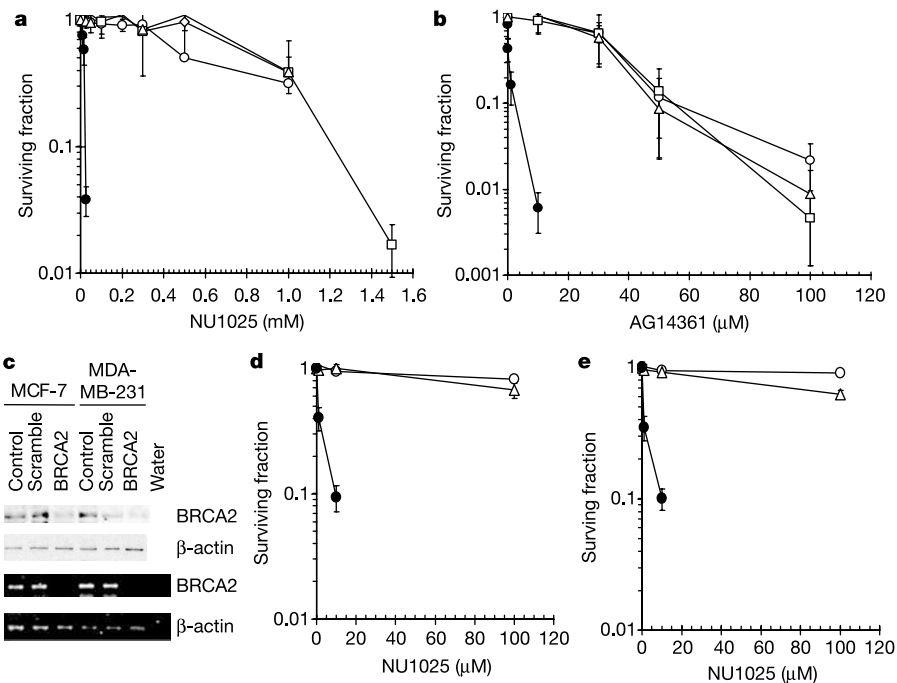
Figure 1 BRCA2-deficient cells are hypersensitive to inhibitors of PARP. **a**, **b**, Colony outgrowth of V79 (wild type; open circles), V-C8 (BRCA2-deficient[14]; filled circles), V-C8#13 (V-C8 complemented with *BRCA2* on human chromosome 13 (ref. 14); squares) and V-C8+B2 (V-C8 complemented with *BRCA2* on an expression vector[14]; triangles) cells upon continuous exposure to the PARP inhibitor NU1025 (**a**) or after a 24-h treatment with AG14361 (**b**). **c**, Western blot and RT–PCR analysis of protein and RNA lysates isolated from MCF-7 (p53^{WT}) or MDA-MB-231 (p53^{mut}) breast cancer cells after 48-h transfection with siRNA. **d**, **e**, Clonogenic survival of siRNA-treated MCF-7 cells (**d**) or MDA-MB-231 cells (**e**) after exposure to the PARP inhibitor NU1025. Open circles, control; triangles, scramble siRNA; filled circles, BRCA2 siRNA. The means and standard deviation of at least three experiments are shown.